JOURNAL OF MATERIALS SCIENCE 29 (1994) 1636–1645

Fibre/matrix interactions in magnesium-based composites containing alumina fibres

FAZAL-UR-REHMAN, S. FOX, H. M. FLOWER, D. R. F. WEST
Department of Materials, Imperial College, London SW7 2BP, UK

An investigation has been made of composites with magnesium-based matrices CPMg, AZ61 and AZ91 reinforced with Safimax low-density (LD), standard-density (SD) and RF Saffil alumina fibres, using either a squeeze or a gas-pressure casting route. Detailed investigations of structural features have been made using SEM, TEM and EDX analysis. The overall extent of reaction between matrix and fibre was affected by the volume fraction of fibres and (locally) by the formation of metal channels between fibre bundles. Fibre microstructure and porosity are the key features which significantly influence the extent of chemical interaction. LD (Safimax) alumina fibres were fully reacted and cannot be employed to produce liquid-metal infiltrated composites, unless a method to stabilize or protect the fibres can be found. In the case of SD Safimax fibres, the metal/ceramic interaction produced a considerable penetration of magnesium into the fibres. However, there was negligible chemical reaction in composites containing RF Saffil alumina fibres.

1. Introduction

Light-alloy metal-matrix composites (MMCs) have assumed increased importance as potential structural materials where weight must be saved. The reinforcement of the metal can remove many of the disadvantages of conventional magnesium-alloys to meet the demands in aircraft, space and automotive applications. The present paper reports the results from a study being carried out to determine preferred matrix/fibre combinations in magnesium-based alloys reinforced with alumina fibres for fabrication by a casting route.

Infiltration of a liquid metal into a die containing a preform of inorganic fibres has been widely used as a method to fabricate MMCs, both for laboratory and commercial developments [1–6]. The production of MMCs by squeeze casting or gas-pressure casting involves three stages. First, the reinforcement is infiltrated by the molten metal. This is followed by pressurization and the final stage comprises the solidification of the metal.

Among the problems which arise in liquid-metal infiltration of fibrous preforms, two are of particular note: (a) inadequate wetting of the preforms by the liquid metal [4–6], (b) excessive interaction between the liquid metal and fibres [7–11]. Both of these problems may degrade mechanical properties of composites. Careful control of casting parameters, alloy additions and coating of fibres can minimize these problems.

Magnesium is 30% lighter than aluminium, has a similar specific strength and specific stiffness (Fig. 1). Magnesium-based composites containing alumina fibres could be preferred over aluminium-based composites because of better specific strength and specific stiffness (the specific strength and specific stiffness values of composites are calculated by the rule of mixtures). The specific strength and specific stiffness of Mg/30% SD alumina fibres should be larger than those of steel. Another advantage of magnesium is its good wetting of most ceramics, compared to aluminium. But it has a disadvantage of being highly reactive with potential reinforcement, including alumina. This, and other factors, results in the actual strength of the composite being far less than the calculated values as discussed in Section 2.

In the present work, magnesium alloys were reinforced with short planar random Saffil (RF) fibres, long aligned Safimax standard-density (SD) and low-density (LD) alumina fibres. Details of the fibres are shown in Table I together with data for other commercially available fibres [7, 12].

2. The influence of interface reaction on mechanical properties

An overview is given here of some of the previous work done on composites. This overview is biased towards the fibre/matrix (F/M) interactions that occur in magnesium-based composites. The interface between fibre and matrix is important in all loading situations where stress is transferred across it. A weak interface will lead to low transverse strength and possibly low modulus in continuous fibre-reinforced material compared to the monolithic metal. As discussed below, longitudinal properties may also be degraded by matrix–fibre interactions; thus control of interface formation is essential.

0022–2461

TABLE I Some characteristics of alumina fibres

Manufacturer	Trade name	Alumina phase	Grain size (μm)	Fibre diameters (μm)	Density (10^{-3} kg m^{-3})	Tensile strength (MPa)	Elastic modulus (GPa)
ICI	SD Safimax	Delta/theta	0.05	3	3.3	2000	250
ICI	LD Safimax	Eta	0.005	3	2.1	2000	207
ICI	RF Saffil	Delta/theta	0.05	3–4	3.3	2000	300
EI DuPont	FP	Alpha	0.5	20	3.8	> 1400	380
ICI	RD	Eta	0.005	3	NA	NA	NA
Nippon	NA	NA	0.05	3	NA	NA	NA

Note: The Safimax and Saffil fibres contain 3%–4% SiO_2; NA, not available.

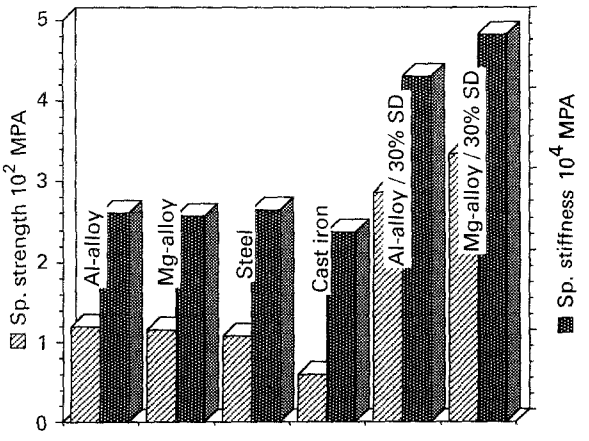

Figure 1 Comparison of materials properties (data taken from [4, 7, 32] and Magnesium Elektron's Data Sheet).

The liquid routes employed in MMC production enhance interfacial reactions due to prolonged contact, at elevated temperatures, between the matrix alloy and the reinforcing material [13]. Further processing or heat treatment may additionally modify the interface [14–18]. Interfacial reactions are evident in almost all MMCs: the interface and the effects of interfacial reactions on the mechanical properties of composites have been widely investigated [5, 7, 13, 14, 17, 18]. Levi *et al.* [15] suggest that a thick reaction zone at the interface is undesirable, especially when it is uneven and rough, as it may have a deleterious effect on the fibre strength and therefore on composite properties [19, 20]. Reeves *et al.* [21] studied the effect of interfacial reaction-layer thickness on fracture of Ti/SiC particulate composites. They reported that the work of fracture of these composites falls from 260 kJ m^{-2} to about 60 kJ m^{-2} with increasing reaction-layer thickness from 0–4 μm.

Many reports on the fracture of fibre-reinforced composites agree that the reaction layer formed at the interface, as a result of chemical reaction, is brittle and fractures at small strains [4, 22–24]. Ochiai and Murakumi [19], presented a theoretical model on the longitudinal strength of fibre-reinforced composites with a brittle reaction zone. They assumed that the fractured reaction layer acts as a circumferential notch around the fibrous reinforcement. They proposed that the strength of the composites is not reduced if the thickness of the reaction zone is below a critical value. In the case of a strongly bonded fibre/brittle zone this value is smaller than in the case of weakly bonded fibre/brittle zone interfaces. If the brittle zone is very thin, the effect of intrinsic defects in the fibre is greater than that of the newly formed notch and the fibre is able to maintain its full strength; as the interaction zone thickens, the interface increasingly begins to dominate the behaviour until a critical point where the fibre fractures simultaneously with the brittle zone. Beyond this critical thickness the zone becomes weaker because it will contain more defects.

They also suggested that the interfaces rely on mechanical interlocking or chemical bonding, or a combination of the two, for load transfer from matrix to the fibres. The interfacial shear strength is thus variable and system specific. Thus the relative strength of the reaction zone itself and its interface with the fibre is of fundamental importance. They verified their model via experimental work on aluminium-based alloys incorporating carbon, boron and silicon carbide fibres. The reported values of critical thickness for carbon, boron and silicon carbide fibres were 0.17, 0.28 and 0.62 μm, and quoted values of fibre diameters were 7, 100 and 100 μm, respectively.

So far only a little work has been done on magnesium-based composites and mostly, it focuses on mechanical properties. In almost all the reports [3, 11, 13, 25–27] the magnesium-based composites had a reaction zone thick enough (e.g. 0.1–0.5 μm in CPMg/FP alumina fibres) to degrade the expected mechanical properties. Hack *et al.* [13, 25] in their work on CP Mg/FP and ZE41A/FP alumina fibre composites, found a reaction zone composed of MgO, 0.14 and 0.28 μm thick, respectively. As they did not report the casting conditions of the composites, it cannot be concluded that the thicker reaction zone was due to alloying. However, a subsequent investigation by Hack *et al.* [27] suggested that the thicker reaction zone in ZE41A was due to larger liquid metal/fibre contact time than that in CPMg/FP alumina fibre composites.

They also found that in the case of CPMg/FP composite, the reaction zone contained MgO particles with a smaller crystallite size than in the case of ZE41A/FP, and effectively forming a continuous layer. They also observed a considerable variation in grain size of the FP alumina fibres. Tensile and fatigue test data were consistent with thicker reaction zones

being weaker, causing a large reduction in tensile properties when the loading was off-axis. They suggested that an increase in interfacial strength brought about either by process modification or through alloying should yield improved off-axis properties. However, an increase in interfacial strength induced by increased F/M reactions is generally accompanied by a decrease in fibre and, subsequently, composite axial properties.

McMinn *et al.* [3] indicated the presence of F/M reaction zone, composed of MgO in ZE41/FP alumina fibre, at three different casting temperatures. They reported that the average MgO particle size was increased with increasing casting temperature, changing from 0.16 μm at 698 °C to 0.30 μm at 755 °C and finally, to 0.37 μm at 810 °C. They suggested that the size of the reaction zone is diffusionally controlled and is dependent on both the actual casting temperature and the time at temperature. They also suggested that the size of the reaction zone cannot simply be used as the true measure of the reaction that occurs to degrade the fibre strength. With the equivalent size of the reaction zone, the composite with larger grain size of the reaction zone would exhibit poorer mechanical properties, as was the case in their study.

Rawal and Misra [26] studied the interfacial bond strength in cast AZ91 alloy reinforced with SiO_2-coated graphite fibres. They observed Mg_2Si and MgO particles together with a few microvoids, formed as a result of reaction between SiO_2 coating and magnesium matrix. They reported, on the basis of mechanical properties test results, and on the SEM observations of the fractured surface which showed limited fibre pull-out, that the interfacial bond integrity is aided by the compressive radial stresses generated due to the difference in the coefficients of thermal expansion of fibre and matrix.

Dinwoodie and Horsfall [28] reported severe binder/matrix reaction in magnesium-based matrix reinforced with RF Saffil alumina fibres containing alumina and silica binders, although no reference to the interface or fibre/matrix reactivity was made. In silica-bonded MMCs most of the castings contained single-phase magnesium-based solid solution as the matrix; the remainder, at the bottom of the composite casting contained a heterogeneous dispersion of Mg_2Si and eutectic Mg/Mg_2Si. A similar effect was observed in the composite with the alumina binder. Increasing amounts of $Mg_{17}Al_{12}$ were identified towards the bottom of the castings.

3. Experimental procedure

Composites 1–5 were produced by gas-pressure casting by the Defence Research Agency, Holten Heath, UK, while composite 6 was produced by Kolbenschmidt, Germany, using a squeeze-casting technique. The fibre preforms were prepared by ICI Runcorn, Cheshire. Although the actual details are regarded as proprietary, an overview of the process is available in the literature [4, 13, 25, 28]. The composites studied are described in Table II.

The casting conditions in terms of melt superheat, fibre preform temperature, pressure and other parameters were similar in composites 1–5. In composite 6 the melt temperature was reported as 670 °C.

Specimens for light and scanning electron microscopy were mounted in bakelite and preground by hand using SiC papers of grit size 400, 800 and 1200, successively. Diamond polishing with 3 and 1 μm diamond suspension was carried out in a conventional manner. Light microscopy was carried out with a Nikon Epiphot microscope. Keller's reagent and standard Baker's solution, were used to reveal matrix and β-phase ($Mg_{17}Al_{12}$), respectively. Scanning electron microscopy (SEM) was carried out on Jeol JSMT200, JSMT220 and JSM35 electron microscopes operating between 20 and 30kV.

X-ray energy-dispersive microanalysis was carried out on lightly etched specimens, which were carbon coated prior to examination. Qualitative and quantitative (ZAF corrected) X-ray microanalysis of the bulk polished and lightly etched samples was carried out using Jeol T200 and JSM35 microscopes respectively.

For thin-foil preparation, the samples 2 mm thick were cut and ground to 200 μm thickness. 3 mm discs were cut by spark erosion, ground to 80–100 μm on SiC paper of 1200 grit size, dimpled down to ~ 25 μm and ion-beam milled to perforation. Multiple thinning was carried out to increase the thin area around the perforation. Quantitative analysis was carried out on Jeol 120 CX and 2000 FX microscopes, operating at 100 and 200 kV, respectively, using Link energy dispersive spectrometers (EDX) and analysis programs.

4. Results

4.1. Infiltration and distribution of fibres

Light microscopy of composites with a relatively low volume fraction ($V_f = 25\%$) of aligned fibres showed fairly large channels of unreinforced metal about 0.05–0.10 mm wide extending throughout the sample,

TABLE II

Composite	Matrix	Alloying elements (wt %)				Reinforcement alumina (Vol %)
		Al	Zn	Mn	Mg	
1	CPMg	0.3	0.2	0	99.5	25 SD Safimax
2	CPMg	0.3	0.2	0	99.5	25 LD/D Safimax
3	CPMg	0.3	0.2	0	99.5	30 SD Safimax
4	AZ61	6.5	1.0	0.15–0.3	Bal.	35 LD Safimax
5	AZ61	6.5	1.0	0.15–0.3	Bal.	35 SD Safimax
6	AZ91	9.0	1.0	0.3	Bal.	20 RF Saffil

along the fibre direction and separating the layers of fibres which composed the preform (Fig. 2a). The bunches of fibres appeared to be pushed back by the flowing melt during infiltration and possibly by growing primary α-magnesium dendrites during solidification. It was noted that the tendency to channel formation was reduced by an increase in volume fraction of fibres. Infiltration of the fibres by metal was very good, despite increased volume fraction of fibres in some composites and only a little porosity could be observed in one sample of CPMg/25% SD fibres. Fig. 2b shows an area at relatively higher magnification from an unreinforced metal channel as in Fig. 2a. In this area large dendrites are clearly visible.

4.2. Fibre matrix interactions in magnesium-based composites

Table III shows bulk analyses of all the composites investigated.

4.2.1. CPMg matrices/alumina fibres

The matrices of CPMg-based composites showed extensive regions of primary α-magnesium dendrites/cells and some lamellar eutectic of α and β-$Mg_{17}Al_{12}$ (Fig. 3a). The bulk analysis in areas containing eutectic had an average aluminum content of about 30% –36% by weight. The volume fraction of eutectic varied with volume fraction of fibres, being (a) higher in composites with low volume fraction of fibres, and (b) higher in composites containing LD alumina fibres rather than SD or RF fibres. CPMg/30% SD exhibited coring, indicating alloying had occurred, but no eutectic structure was observed.

The matrix in unreinforced regions in the metal channels between the fibre bunches showed large dendrites of magnesium (Fig. 3b) while the area between the fibres had smaller dendrites/cells. This refinement of dendrites was observed to start a short distance into the reinforced region. The dendritic growth was marked in low volume fraction fibre composites. In CPMg/30% SD alumina fibres, a few large Mg_2Si particles were also found, as shown in the transmission electron micrograph in Fig. 4. The composite CPMg/25% LD alumina showed the debonding of fibres, which probably occurred during polishing (Fig. 5). The fibres were completely conver-

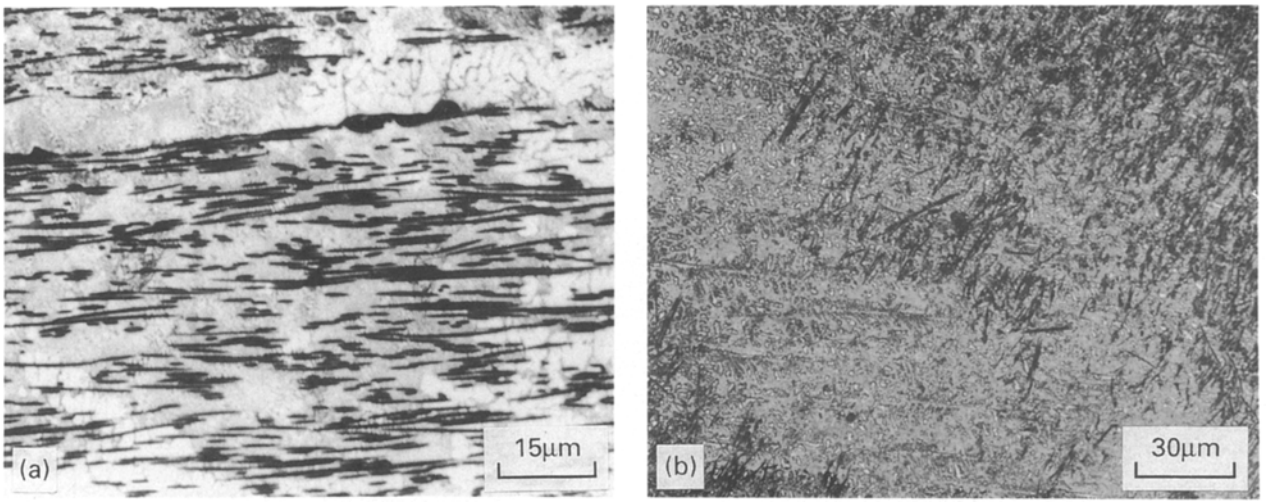

Figure 2 (a) Light micrograph showing a large channel of unreinforced metal in CPMg/25% SD; (b) Light micrograph of CPMg/25% LD showing dendrites in an unreinforced channel.

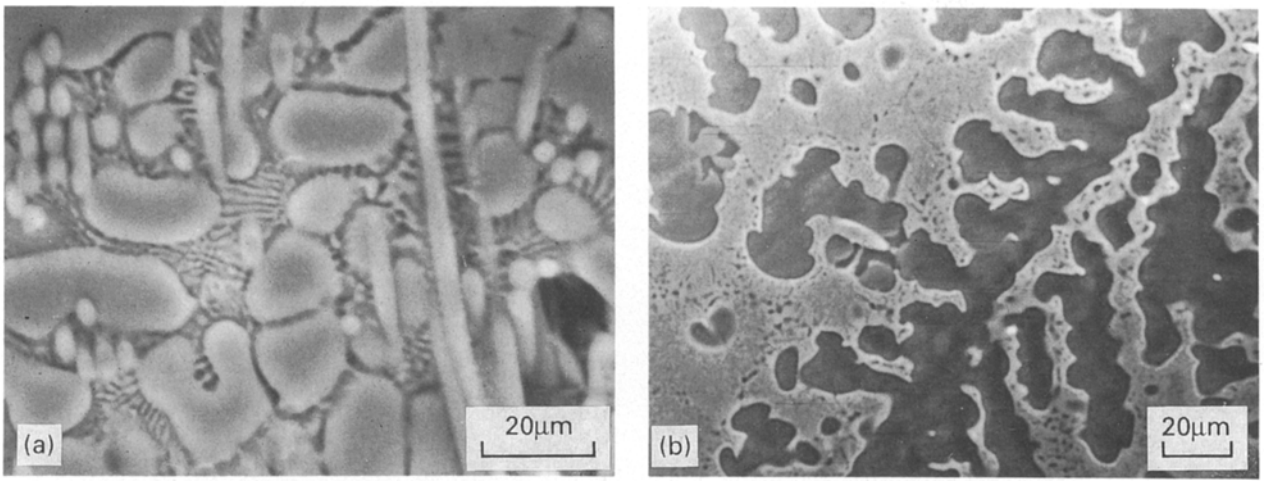

Figure 3 (a) Scanning electron micrograph CPMg/25% SD showing two types of matrix structures; α-magnesium cells and eutectic of α + β, and fibres; (b) scanning electron image of CPMg/25% SD, showing a large α-magnesium dendrite surrounded by a fine eutectic of α + β.

TABLE III

Composite	Elements (wt %, average values)				
	Mg	Al	Zn	Si	Oxygen (by stoichiometry)
1 AZ91/20%RF α–Mat[a]	95.3	4.0	0.6	0.1	–
Coring	85.3	14.1	0.6	–	–
Eutectic	68.0	30.8	0.8	0.4	–
Fibre[b]	–	51.3	0.2	1.9	46.6
2 AZ61/35%SD α–Mat	92.1	7.3	0.5	0.1	–
Coring	79.0	19.2	1.0	0.8	–
Eutectic	67.8	28.7	3.3	0.2	–
Fibre	28.7	30.8	0	0.2	43.3
3 CPMg/30%SD α–Mat	99.7	0.3	0	0	–
Coring	77.3	21.6	0.1	1.0	–
Fibre	30.1	25.8	0.1	1.0	43.0
4 CPMg/25%SD α–Mat	99.7	0	0.3	0	–
Eutectic	63.8	35.9	0.1	0.2	–
Fibre	43.0	13.4	0.1	0.1	43.4
5 AZ61/35%LD α–Mat	87.0	12.5	0.5	0	–
Coring	77.2	22.5	0.1	0.2	–
Eutectic	68.3	31.5	0.1	0.1	–
Fibre	53.8	5.1	0.5	0.1	40.5
6 CPMg/25%LD α–Mat	96.5	3.5	0	0	–
Eutectic	69.7	30.1	0.1	0.1	–
Fibre	58.8	1.0	0	0.1	40.1

[a] Central regions of α-Mn dendrite/cells.
[b] For fibres the analysis were carried out at the centre of the fibres.

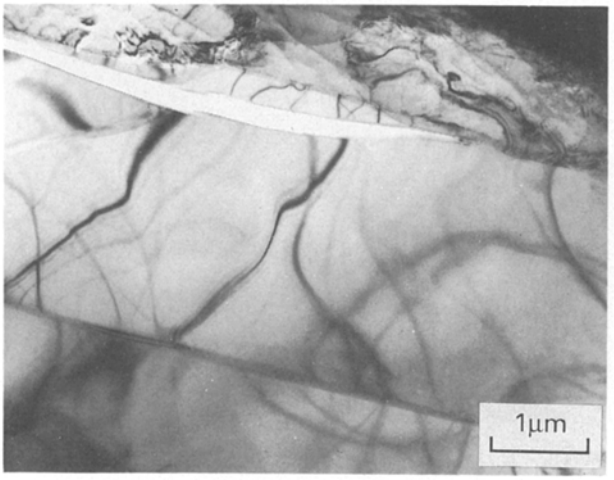

Figure 4 Transmission electron image of a Mg_2Si particle found in CPMg/30% SD.

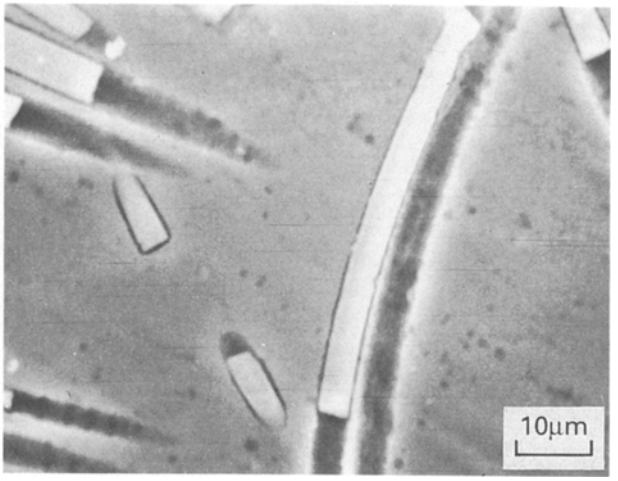

Figure 5 Scanning electron image of CPMg/25% LD showing debonded fibres.

ted into MgO as a result of chemical interaction between the fibre and the matrix metal.

4.2.2. Composites containing AZ61 and AZ91 matrices

Fig. 6 shows a typical light micrograph of composite containing AZ61 and AZ91 alloys. This micrograph shows light areas representing the central regions of primary magnesium dendrites/cells; there is a surrounding darker area which contains small particles of β-phase. Eutectic is visible in some areas. There is another lighter layer in between the darker region and the fibre. As shown in Table III, the EDX bulk analyses of these magnesium alloy-based composites containing aluminium and zinc showed 4–7 wt% Al, 0.5–0.6 wt% Zn, 0–0.1 wt % Si within the large central lighter areas of primary magnesium in the matrix, and also in the very small lighter areas between the fibres and the darker region. The analysis data show that the central light areas of primary magnesium cells/dendrites sometimes show detectable variations in aluminium content, i.e they show some coring.

The dark areas represent a substantial coring effect and contain 14–22 wt % Al, 0.1–1.0 wt % Zn and 0–0.8 wt % Si. The eutectic structure contained 28.7–31.0 wt % Al and 0.1–3.3 wt % Zn and 0.15–0.4 wt %Si. The amount of eutectic was relatively large in AZ61/35% LD fibres composites, as compared to that in AZ61/35% SD or AZ91/20% RF composites, which was probably due to change in matrix chemistry as a result of chemical reaction

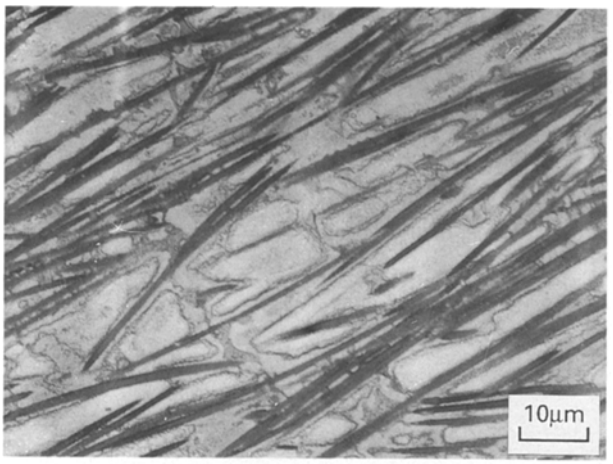

Figure 6 Light micrograph showing primary magnesium dendrite/cell with dark areas containing α-magnesium with some β-phase, a eutectic structure and some primary magnesium nucleation at the fibre surface.

between fibre and matrix. As shown in Table III, there is more aluminium left in the fibre in AZ61/35% LD than that in CPMg/25% LD. This reduction in the extent of chemical reaction, if measured in terms of remaining aluminium content of fibres, is the combined effect of matrix alloy and fibre volume fraction. This effect is more pronounced in AZ61/35% SD and CPMg/25% SD composites.

4.2.3. Reinforcement interaction with the matrix

As noted above, the presence of fibres reduces the dendrite/cell size in the matrix. More importantly, both low-density (LD) and standard-density (SD) alumina fibres were attacked by magnesium melts. However, the degree of interaction is dependent upon fibre type. Low-density (LD) η-alumina fibres had undergone extensive chemical interactions while standard-density (SD) fibres had reacted to a lesser extent. The massive penetration of magnesium into LD fibres and its chemical interaction with η-alumina totally changed the fibre microstructure (Fig. 7). The TEM image of the virgin LD fibre is presented in Fig. 8 for comparison. The grain size of virgin LD fibre is ~ 0.005 μm, with a large amount of porosity, mostly interconnected. It should be noted that the crystallite size of the fibre had increased to around 0.1 μm and the EDX analysis showed the presence of 58.8 wt% Mg with only 1.0 wt% Al in the centre of the fibre (balance oxygen). A SADP of the fibre centre was indexed as MgO, i.e. the fibre has been totally converted from alumina to magnesia.

Fig. 9 shows a high-magnification transmission electron micrograph of AZ91/RF Saffil, together with its composition profile across the interface. The matrix area adjacent to the fibre containing primary α-magnesium had 9–10 wt% Al, 0.2–0.4 wt% Zn, balance magnesium, and clearly shows a sharp F/M interface with no visible interaction zone. Some particles are seen, however, on the fibre surface. The fine particles nucleated at the interface are MgO; the EDX analysis

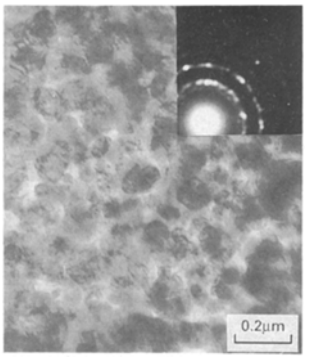

Figure 7 A transmission electron image of a fibre from CPMg/25% LD.

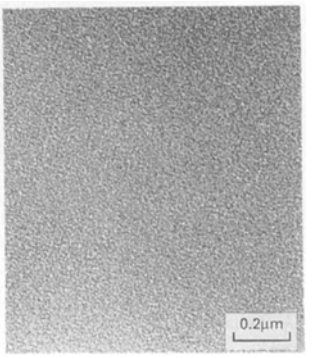

Figure 8 A transmission electron image of a virgin LD Safimax alumina fibre.

showed 57.2 wt% Mg, balance oxygen. The fibre surface appeared to be smooth, compared to that in other composites, and the fibre itself remained microstructurally and chemically mainly δ-alumina (identified from SADP inset) with bulk of the fibre. The EDX analysis of the fibre showed 0.2 wt% Mg at the interface but zero at a depth of 0.1 μm inside the fibre. In comparison, Fig. 10 shows CPMg/25% LD alumina fibres and its composition profile. The EDX analysis showed complete conversion of the fibre to MgO and dissolution of aluminium from the fibre into the magnesium matrix.

5. Discussion

5.1. Infiltration

The infiltration of fibres by liquid magnesium was complete in all the composites. The distribution of fibres was almost uniform in the composites with high volume fraction ($V_f = 35\%$) of fibres, while in the composites with low volume fraction ($V_f = 25\%$) of fibres, large channels of unreinforced metal could be seen. This affected the local volume fraction of fibres. In this case, either the fibres were pushed back by the fluid flow during infiltration and by the growing primary dendrites of α-magnesium during solidification of the melt, or the fibres were not uniformly distributed during preform production.

5.2. The effect of matrix chemistry

The large amount of eutectic of α and β-$Mg_{17}Al_{12}$ observed in composites containing CPMg matrices

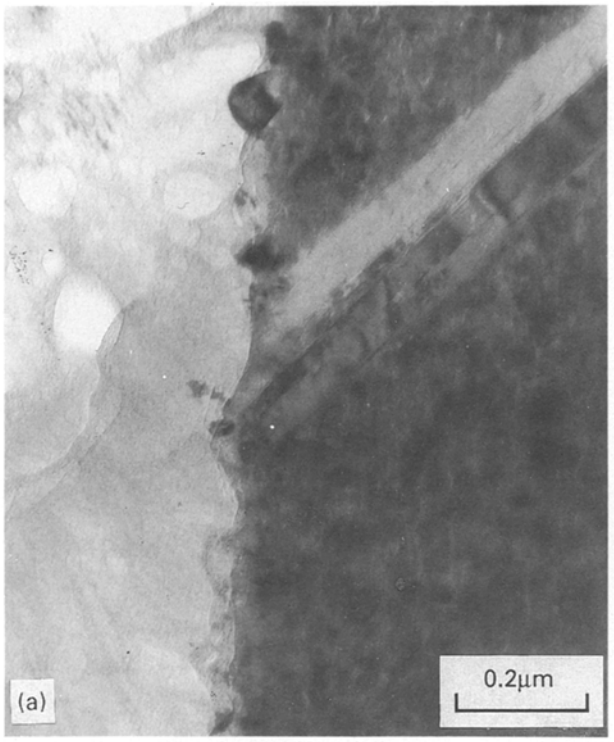

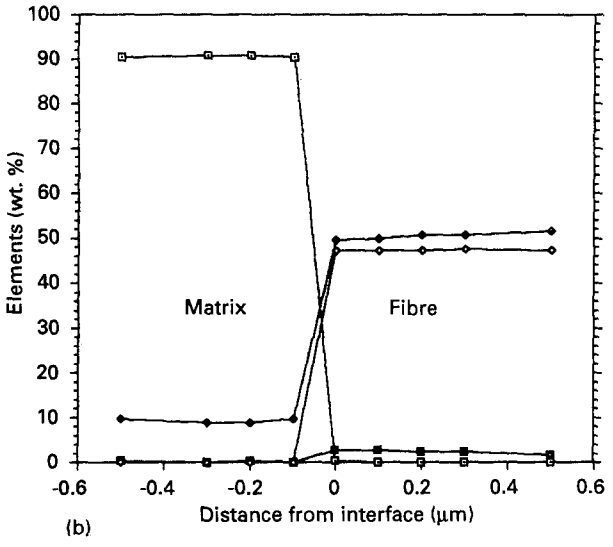

Figure 9 (a) A transmission electron image of AZ91/20% RF Saffil fibres; (b) the corresponding elemental concentration profile across the fibre/matrix interface. (□) Mg, (◆) AL, (■) others, (◇) oxygen.

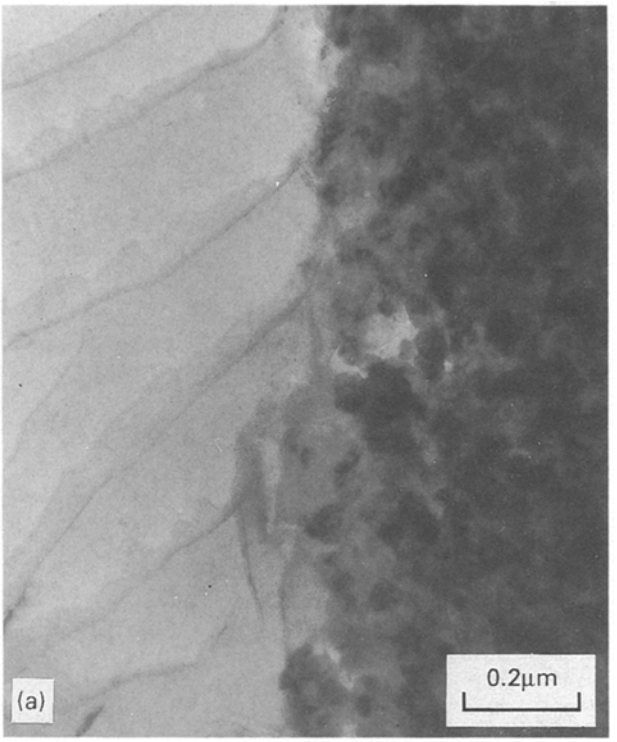

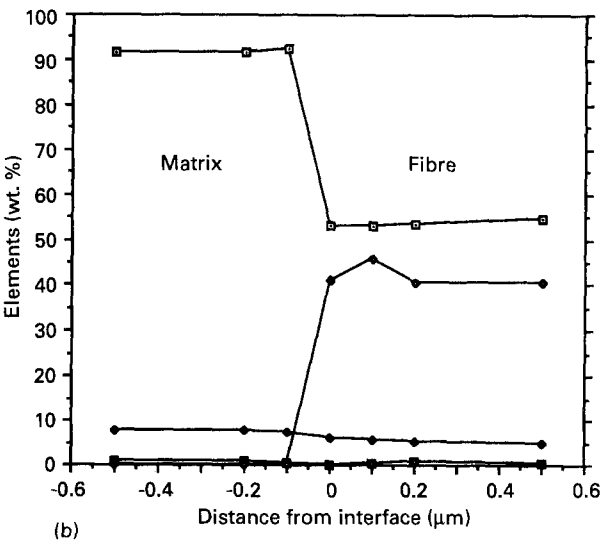

Figure 10 (a) Transmission electron image of CPMg/25% LD; (b) the corresponding elemental concentration profile across the interface. (□) Mg, (◆) AL, (■) others, (◇) oxygen.

was formed as a result of extensive fibre/matrix (F/M) interactions and massive transfer of magnesium and aluminium across the interface. The matrices of the composites infiltrated with commercially pure magnesium had a significantly increased aluminium content as a result of F/M interactions. This increase was so large in some areas that a large volume fraction of eutectic of α and β-phase containing an average of 32.5 wt % Al was observed. The amount of eutectic varied in different composites depending on the extent of chemical reaction, i.e. larger in CPMg/LD fibres and relatively smaller in CPMg/SD fibres.

The composites containing aluminium and zinc in the matrix alloy had three types of matrix constituents/or structure: light regions of primary α-magnesium with 4–12.5 wt % Al, dark areas of α-magnesium with very fine β-phase containing 14–22.5 wt % Al and a eutectic of α and β with 29–36 wt % Al. The dark regions of the matrix show high aluminium content indicating considerable microsegregation. However, these aluminium contents are substantially in excess of the equilibrium solid solubility of aluminium in magnesium, which is 12.5 wt % at the eutectic temperature. The width of these areas is less than a micrometre and, bearing in mind the interaction volume in EDX, it is possible that some areas of eutectic are picked up. The analysed values of eutectic areas lie in the range of 29–36 wt % Al, which is in reasonable agreement with the binary phase diagram value of the Mg–Al system, which is 33 wt % Al [29].

The large variation in matrix chemistry could be attributed to the solidification behaviour of the matrix

alloy cast under pressure and is discussed in the section on solidification. The matrix alloy containing aluminium and zinc had been the least reactive. Although the reduction in F/M interaction can be partially related to fibre type and volume fraction, these data indicate that an increase in aluminium content in the magnesium alloy used as a matrix reduces the F/M interactions during composite production.

5.3. Thermodynamics and kinetics

The Gibb's free energy, the driving force for the reduction of alumina by the magnesium melt, is given by [30, 31]

$$3Mg(l) + Al_2O_3(s) = 3MgO(s) + 2Al(l)$$

$$\Delta G_0 = 405\,760 + 3.75T \log T - 87.64T \text{ cal} \quad (1)$$

which is -668.36 kJ mol^{-1} at 670 °C (The reported melt temperature of one of the composites was 670 °C. This is used for calculations. ΔG values are per mole of oxygen).

Thus there is a considerable thermodynamic driving force of free energy which can promote the formation of MgO. It is unlikely to be significantly reduced by lowering the activity of magnesium by alloying with relatively small amounts of aluminium, as in the alloys used here. The equilibrium activity of magnesium (a_{Mg}) changes almost linearly with the addition of aluminum and is ~ 0.89 for AZ91. Only at a magnesium concentration of 0.9 wt % in aluminium, does the activity of magnesium fall to such a low value that the stability of oxides of magnesium and aluminium is reversed [32]. A thermodynamic driving force for reaction thus exists for all the matrix alloys analysed here. However, the degree of reaction is governed by the kinetics of the process. Thus the rate of reaction would be dependent on the transport of the reactant (magnesium) into the fibre and the reaction product (aluminium) out of the fibre. An increase in aluminium content of the matrix alloy would be expected to decrease the concentration gradient across the interface. This should be expected to reduce the rate of reaction by reducing the transport of the reactants and products [33].

The presence of Mg_2Si in CPMg/30% SD fibres results from a chemical reaction between the SiO_2 (from the binder and fibre) and the magnesium-rich CPMg matrix. Possible chemical reactions between magnesium and SiO_2 are as follows

$$2Mg(l) + SiO_2(s) = 2MgO(s) + Si(s)$$

$$\Delta G_{670}\,^{\circ}C = -317.98 \text{ kJ mol}^{-1} \quad (2)$$

$$2Mg(l) + 2SiO_2(s) = Mg_2SiO_4(s) + Si(s)$$

$$\Delta G_{670}\,^{\circ}C = -435.22 \text{ kJ mol}^{-1} \quad (3)$$

$$4Mg(l) + 2SiO_2(s) = 2Mg_2SiO_3(s) + Si(s)$$

$$\Delta G_{670}\,^{\circ}C = -435.22 \text{ kJ mol}^{-1} \quad (4)$$

$$4Mg(l) + SiO_2(s) = Mg_2Si(s) + 2MgO(s)$$

$$\Delta G_{670}\,^{\circ}C = -379.49 \text{ kJ mol}^{-1} \quad (5)$$

where s indicates solid and l liquid.

Although these chemical reactions are all thermodynamically possible, EDX analysis suggests that the reaction process promotes the formation of Mg_2Si and MgO as in Equation 5. Rawal and Misra [34] also observed Mg_2Si particles in a graphite/magnesium composite, mixed with oxide particles at the interface. They suggested that the mixed oxide and silicide phases at the interface form a graded junction and ensure good bonding between magnesium and fibres.

In the present study, very large primary Mg_2Si particles are formed in the matrix attributable to high localized concentrations of silicon. These particles showed a tendency to segregate, which might be expected to have an adverse effect on the mechanical properties.

5.4. Solidification behaviour

The CPMg-based composites containing either 25% SD or 25% LD alumina fibres (by volume) showed two features of matrix morphology, i.e. primary magnesium dendrites nucleated away from fibre surface and a lamellar eutectic of α-magnesium and $\beta(Mg_{17}Al_{12})$. The growth of the lamellae is perturbed by the fibres in these composites as the lamellae seem to avoid the fibres as two solidifying dendrites avoid each other (Fig. 3a). In the CPMg-based composite with 30% by volume of SD fibres, the eutectic formation was more limited. In magnesium-based composites containing aluminium and zinc (Fig. 6) the solidification probably started mainly in the interfibre region rather than at the fibre/melt interface. However, a very thin layer of primary magnesium, appearing light between the fibres and coring pattern, was also observed with an aluminium content of 4–12.5 wt %. This suggests that the fibres did induce some nucleation perhaps at a later stage as significant chemical reaction of fibres was also observed in the reacted fibre composites.

Li *et al.* [35] have reported similar matrix structures, i.e. primary dendrites/cells with associated coring on the basis of their study on Al–6 wt % Cu/SD alumina fibres, under controlled solidification conditions. They observed a minimum copper content at the start of solidification and a rapid increase in copper content in the later stage of freezing. They also reported that the matrix microstructure and microsegregation varied significantly, with change in total solidification time, θ_t. The final solidified microstructure was cellular, when $\theta_t > 10$ s and the last liquid to solidify is located predominantly around the fibres giving a layer of intermetallic $CuAl_2$ at the interface. The matrix structure was dendritic at $\theta_t \sim 1$ s with more dispersed intermetallic $CuAl_2$. They observed a more uniform matrix composition at a larger solidification time of 520 s. They suggested that the back diffusion of solute in the solid α-aluminium phase was responsible for that when the concentration gradient grew steeper at the solid–liquid interface.

In a recent review paper, Mortensen and Jin [36] explained the dendrite/cell formation by two mechanisms: dendrite arm ripening, wherein smaller arms

remelt to deposit on to larger ones, and dendrite arm coalescence, which gradually erases the dendritic character of the solid metal. However, they did not observe any chemical reaction between matrix and fibre in their case. while in the present case F/M interactions had drastically changed local concentrations of solute and thus had an effect on the final solidified microstructure, which resulted in eutectic structure, microsegregations and primary magnesium dendrites or cells with large variations in chemical composition, as shown in Table III.

5.5. The effect of reinforcement

There are major differences in the extent of F/M interaction as shown by the observed aluminium content of the matrices and the magnesium content of fibres in Table III. From the data presented, the extent of chemical reaction can be mainly attributed to fibre type, and to a large degree, fibre volume fractions. Considering the reaction in terms of diffusion across the interface, the penetration of magnesium into fully dense alumina, if limited by the bulk oxide diffusion rate, is calculated to be only 0.002 μm, using diffusion data [34]. In all cases, including the case of RF Saffil fibres, the penetration of magnesium into fibres was far too great for bulk diffusion in alumina to be responsible. Hence the features to be considered are fibre porosity (its volume fraction, distribution and nature, e.g. interconnected or closed), other short circuit diffusion paths, e.g. boundary diffusion (fine crystallite size favouring diffusion) and the occurrence of exothermic reactions.

Porosity is expected to be particularly significant, although its effect cannot be entirely separated from other features. Saffil RF alumina fibres with 50 nm grain size and very low density of pores, many not interconnected, had least reacted surfaces. Also, some of the RF Saffil fibres contained no surface porosity. This would naturally be expected to block the way of any metal penetration. As a result, a maximum of 0.05 μm thick reaction zone was observed in composite containing RF Saffil alumina fibres. SD fibre is chemically, crystallographically and microstructurally similar to RF grade and is expected to show a similarly limited reaction zone. However, the suppliers indicated that this batch of SD fibres may have had a large amount of interconnected porosity (usually a characteristic of LD fibres, Table I), which was responsible for increased chemical reactions. LD η-alumina is less thermodynamically stable than SD and RF δ-alumina and this could also contribute to the higher reactivity of LD fibres. However, a higher volume fraction of interconnected porosity and much smaller crystallite size (0.005 μm) must be the primary factors responsible for the very much greater degree of chemical reaction observed in this case, resulting in complete conversion of fibre to MgO. The exothermic nature of this reaction also results in heat evolution which would prolong the liquid metal/fibre contact time, hence giving more chance for remelting of any solidified metal, further infiltration of pores and increased interaction which ultimately converted the alumina fibres of 0.005 μm crystallite size to MgO of 0.1 μm crystallite size.

An increase in fibre volume fractions has significantly affected the extent of chemical reaction. The effect of fibre volume fraction is very important, particularly when the fibre preform temperature is below the melt temperature. A higher volume fraction of fibres would be expected to have a relatively more chilling effect on the infiltration front, thereby promoting fibre-induced nucleation of the primary matrix due to increased cooling of the liquid metal in the vicinity of the fibres. This would ultimately result in lowering of fibre/liquid metal contact time and thus reducing chemical reaction.

6. Conclusions

1. The composites with the lowest volume fraction of fibres had the largest unreinforced metal channels.
2. An increase in fibre volume fraction of fibres in any composite reduces the fibre/matrix interactions.
3. Fibre/matrix interactions are critically dependent upon fibre type and microstructure; large (0.05 μm) grain-size RF alumina fibre with little porosity, of limited connectivity, reacted least, while small (0.005 μm) grain-size LD alumina fibre with high volume fraction of connected porosity reacted completely with magnesium.
4. There is evidence that increasing the aluminum content of the magnesium alloy used as a matrix reduces the degree of chemical reaction between matrix and fibres.

Acknowledgement

This study has been funded by a BRITE-EURAM programme. The authors are grateful to Drs A. M. Walker and M. H. Stacey, Imperial Chemical Industries, DRA Holten Heath, UK, and to Kolbenschmidt, FRG, for providing material support. One of the authors (F. Rehman) thanks the Government of Pakistan for partial funding.

References

1. A. MORTENSEN, L. J. MASUR, J. A. CORNIE and M. C. FLEMINGS, *Metall. Trans.* **20A** (1989) 2535.
2. L. J. MASUR, A. MORTENSEN, J. A. CORNIE and M. C. FLEMINGS, *ibid.* **20A** (1989) 2548.
3. A. McMINN, R. A. PAGE and W. WEI, *ibid.* **18A** (1987) 273.
4. T. W. CLYNE, M. G. BADER, G. R. CAPPLEMAN and P. A. HUBERT, *J. Mater. Sci.* **20** (1985) 85.
5. T. W. CLYNE, in "Proceedings of ICCM6-ECCM2", edited by F. L. Matthews (Elsevier Applied Science, London, 1987) pp. 275–85.
6. J. M. CHIOU and D. D. L. CHUNG, *J. Mater. Sci* **26** (1991) 2583.
7. S. FOX, H. M. FLOWER and D. R. F. WEST, unpublished work (1989–90).
8. D. J. TOWLE and C. M. FRIEND, *J. Mater. Sci.* **27** (1991) 2781.
9. C. R. CAPPLEMAN, J. F. WATTS and T. W. CLYNE, *ibid.* **20** (1985) 2159.
10. M. FISHKIS, *ibid.* **26** (1991) 2651.
11. M. PFIEFER, J. M. RIGSBEE and K. K. CHAWLA, *ibid.* **25** (1990) 1563.
12. M. H. STACEY, *Mater. Sci. Technol.* **4** (1984) 227.

13. J. E. HACK, R. A. PAGE and G. R. LEVERANT, *Metall. Trans.* **15A** (1984) 1389.
14. S. J. SWINDLEHURST and I. W. HALL, in "Proceedings of the International Symposium on Cast Reinforced MMCs", edited by S. G. FISHMAN and A. K. DHINGRA, (ASM, 1988) pp. 281–7.
15. C. J. LEVI, G. J. ABASCHIAN and R. MEHRABIAN, *Metall. Trans.* **9A** (1978) 697.
16. K. U. KAINER, *Mater. Sci. Eng.* **A135** (1991) 243.
17. A. MAGATA and I. W. HALL, *J. Mater. Sci.* **24** (1989) 1959.
18. C. S. LEE, J. M. RIGSBEE, K. K. CHAWLA and M. PFIEFER, in "Proceedings of the International Symposium on Cast Reinforced MMCs", edited by S. G. FISHMAN and A. K. DHINGRA (ASM, 1988) pp. 301–7.
19. S. OCHIAI and Y. MURAKUMI, *J. Mater. Sci.* **14** (1979) 831.
20. A. G. METCALFE and M. J. KLEIN. *Compos. Mater.* **1** (1974) 125.
21. A. J. REEVES, H. DUNLOP and T. W. CLYNE, *Metall. Trans.* **23A** (1992) 977.
22. P. W. PETRASEK and J. W. WEETON, *Trans. Metall. Soc. AIME* **230** (1964) 977.
23. D. W. HEITMAN, L. A. SHEPARD and T. H. COURTNEY, *J. Mech. Phys. Solids* **21** (1973) 75.
24. S. OCHIAI, M. MIZUHARA and Y. MURAKUMI, *J. Jpn. Inst. Metals* **37** (1973) 208.
25. J. E. HACK, R. A. PAGE and G. R. LEVERANT, *ibid.* **15A** (1984) 1397.
26. S. P..RAWAL and M. S. MISRA, in "Proceedings of ICCM6-ECCM2", Vol. 2, edited by F. L. Matthews (Elsevier Applied Science, London, 1987) pp. 169–82.
27. J. E. HACK, R. A. PAGE and R. SHERMAN, *ibid.*, Vol 16A, pp. 2069–77.
28. J. DINWOODIE and I. HORSFALL, *ibid.*, Vol. 2., pp. 390–401.
29. J. L. MURRAY, *J. Bull. Alloy Phase Diag.* **3** (1) (1982) 60.
30. E. T. TURKDOGAN, "Physics and Chemistry of High Temperature Technology" (Academic Press, London, 1980).
31. O. KUBACHEWSKI and C. B. ALCOCK, "Metallurgical Thermochemistry", 5th Edn, (Pergamon, London, 1979) pp. 378, 381–382.
32. S. FOX, H. M. FLOWER and D. R. F. WEST, "Proceedings of ECCM-4", September 1990, Stuggart, FRG.
33. W. D. KINGERY, H. K. BOWEN and D. R. UHLMANN, "Introduction to ceramics", 2nd Edn. (Wiley, Lond., 1986) pp. 240, 385–90, 407–11.
34. S. P. RAWAL and M. S. MISRA, in "Proceedings of Interfaces in Polymer, Ceramic and MMCs", edited by H. Ishida (Elsevier Applied Science, New York, 1988) 179–87.
35. Q. F. Li, D. G. McCARTNEY and A. M. WALKER, *J. Mater. Sci.* **26** (1991) 3565.
36. A. MORTENSEN and I. JIN, *Int. Mater. Rev.* **37** (2) (1992) 101.

Received 25 March
and accepted 8 June 1993